

Energetic and Kinematic Properties of Recurrent Solar Active Region Jets: Multi-Wavelength Analysis with AIA and IRIS Observations

Prakhar Singh^{1,2}, Dr. Vaibhav Pant¹, Dr. Arpit K Shrivastav¹

¹ Aryabhata Research Institute of Observational Sciences (ARIES), Nainital, India

² Indian Institute of Technology Roorkee (IITR), Roorkee, India



Abstract

We analyze recurrent solar jets observed on 6 March 2022 near active region NOAA 12960 using SDO/AIA and IRIS data. Jets were examined across AIA passbands and IRIS spectral channels to investigate their dynamics and energetics. Kinematic properties (length, width, duration, velocity), mean temperature, and electron density were determined using the DEM technique and O IV 1399.77/1401.16 Å intensity ratios. Energy flux components, including kinetic, potential, enthalpy, and radiative fluxes, were estimated, revealing that kinetic and enthalpy fluxes dominate the energy budget, emphasizing their significant role in jet dynamics.

Introduction

- ☐ Solar jets are dynamic, collimated plasma ejections along straight / obliqued magnetic field lines.
- ☐ Small-scale dynamic activities observed in multiple wavelengths, showcasing their multi-thermal nature across various solar atmospheric layers.
- ☐ Jets play a crucial role in transferring mass and energy through the solar atmosphere.
- ☐ Crucial for understanding magnetic reconnection, plasma heating, solar wind acceleration, and their impact on solar dynamics and space weather.

Observation and Data

- ☐ Our analysis focuses on four distinct solar jets observed near the active region NOAA 12960 on 06 March 2022 from 21:59 UT to 23:54 UT.
- ☐ We utilize the observations from Atmospheric Imaging Assembly (AIA) and Interface Region Imaging Spectrograph (IRIS)

Interface Region Imaging Spectrograph (IRIS)

Imaging data used from 2 channels - 1400 Å and 2796 Å (Slit-Jaw Imager (SJI) FUV2 Spectral Channel (Si IV 1403 Å)

Atmospheric Imaging Assembly (AIA) /Solar Dynamic Observatory(SDO)

Imaging data used from 6 EUV Channels - 94Å, 131Å,171Å,193Å, 211Å, 335Å

Methodology and Analysis

Slit is fixed along the jet, and plasma motion is tracked by observing the leading edge of the jet. (refer to Fig 1 and Fig 2)

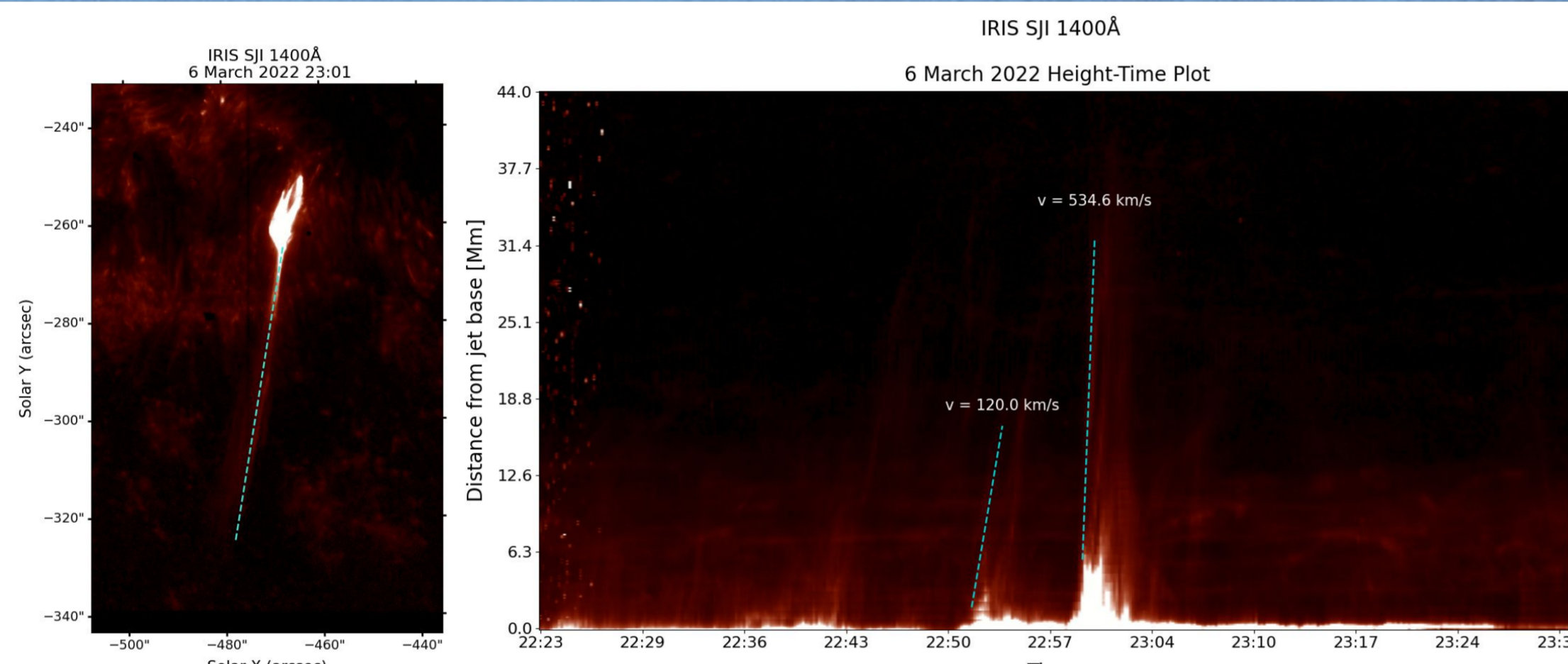


Figure 1: Position of slit along the spire for jet J2b.

Figure 2: Height-Time plot from the slit chosen to deduce the velocity for jet J2(a,b) for 1400 Å

- ☐ Physical parameters of jets (length, width, duration, velocity) were deduced using the time-distance method for IRIS (1400 Å, 2796 Å) and AIA (171 Å) channels. (refer Table 1)

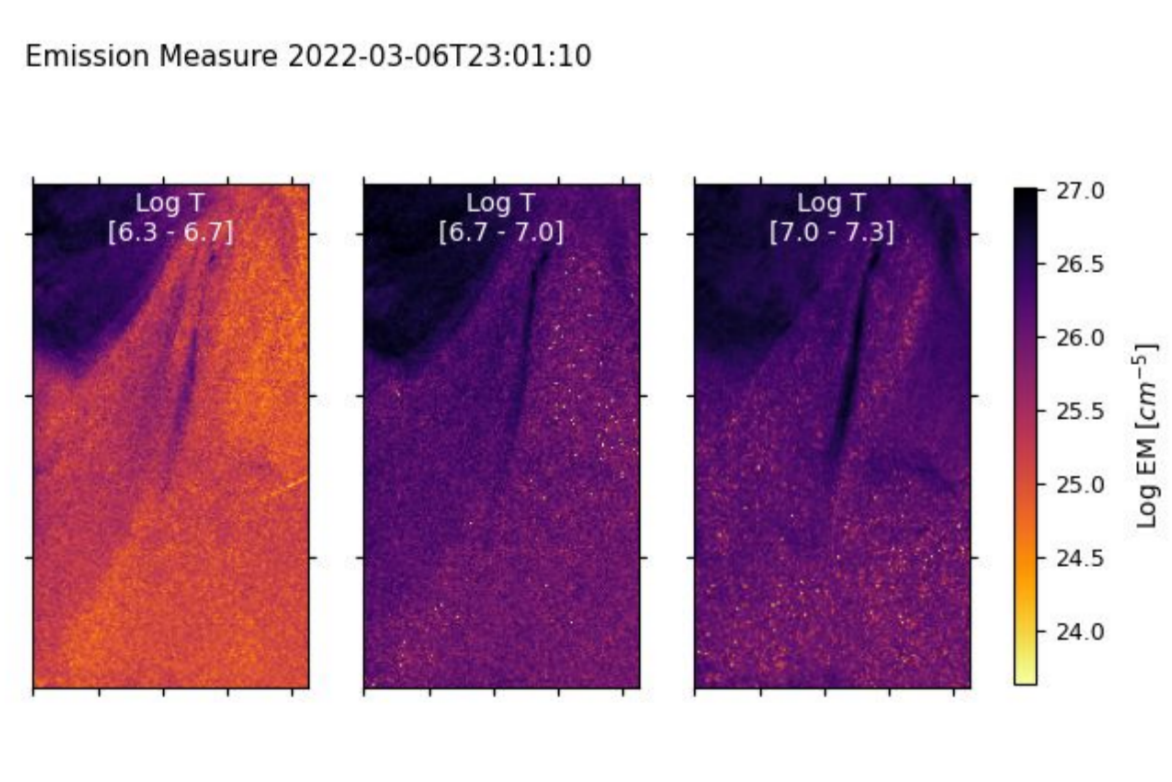


Figure 3: Emission measure map for different temperature bins for jet J2b.

DEM analysis (Hannah & Kontar) applied on six AIA EUV channels (94 Å, 131 Å, 171 Å, 193 Å, 211 Å, 335 Å) to extract plasma parameters such as emission measure, EM-weighted temperature, and electron density.

- ☐ Using the calculated parameters (length, velocity, electron density, and temperature), we estimate the energy fluxes associated with the plasma ejection (refer table 2).

We constructed a time-series map using IRIS spectral data of jet J2b, observing the signatures of the O IV (1399.77 Å) and O IV (1401.16 Å) lines (Fig 4).

Using the intensity ratio of these two lines, we derived the electron density within the region of interest (Fig. 5).

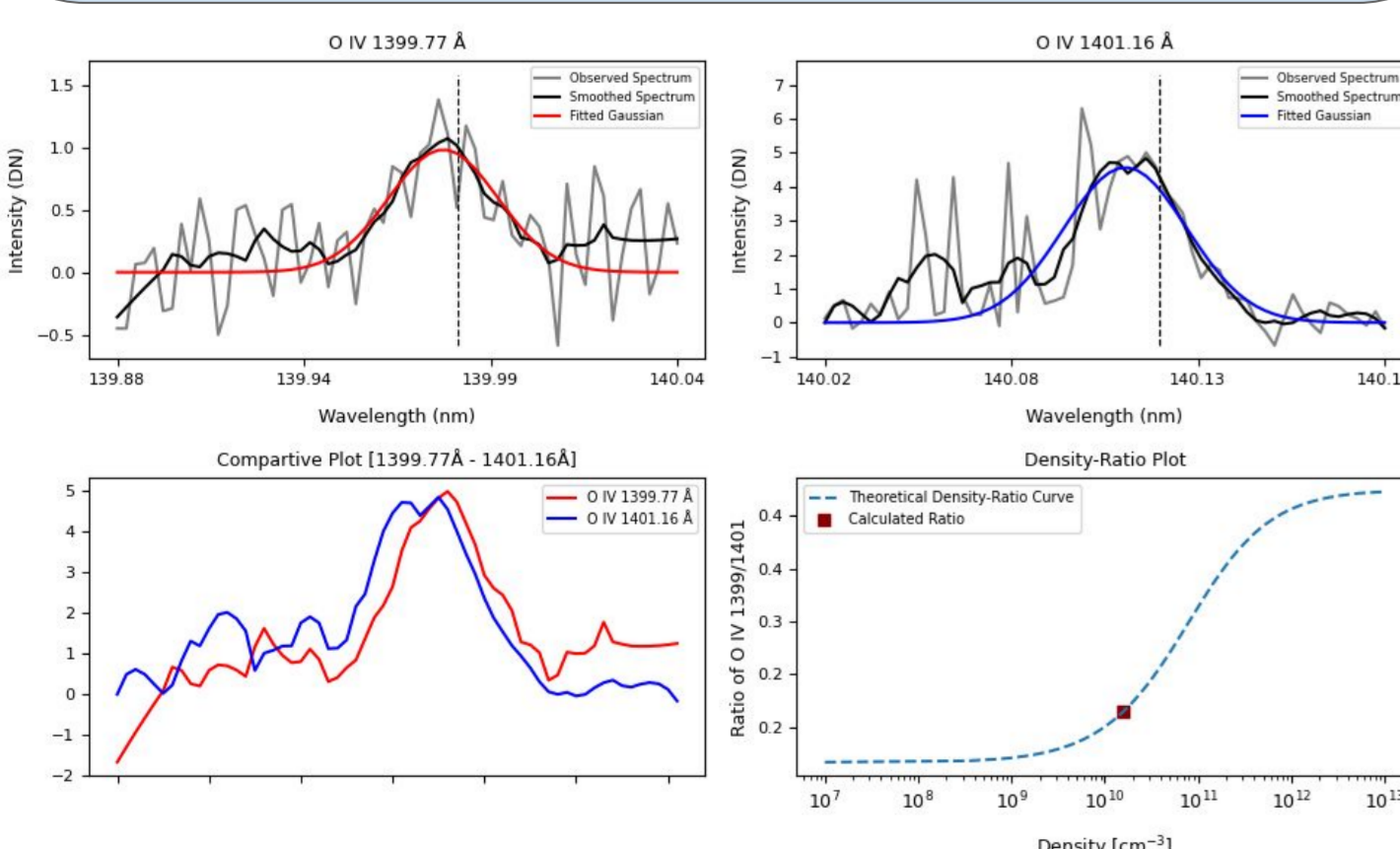


Figure 5: (a-b) O IV 1399.77 Å and O IV 1399.77 Å spectral profile, (c) Comparative plot of O IV doublet (with O IV 1399.77 Å multiplied by ratio) and (d) electron density corresponding to ratio value on Theoretical R-D plot.

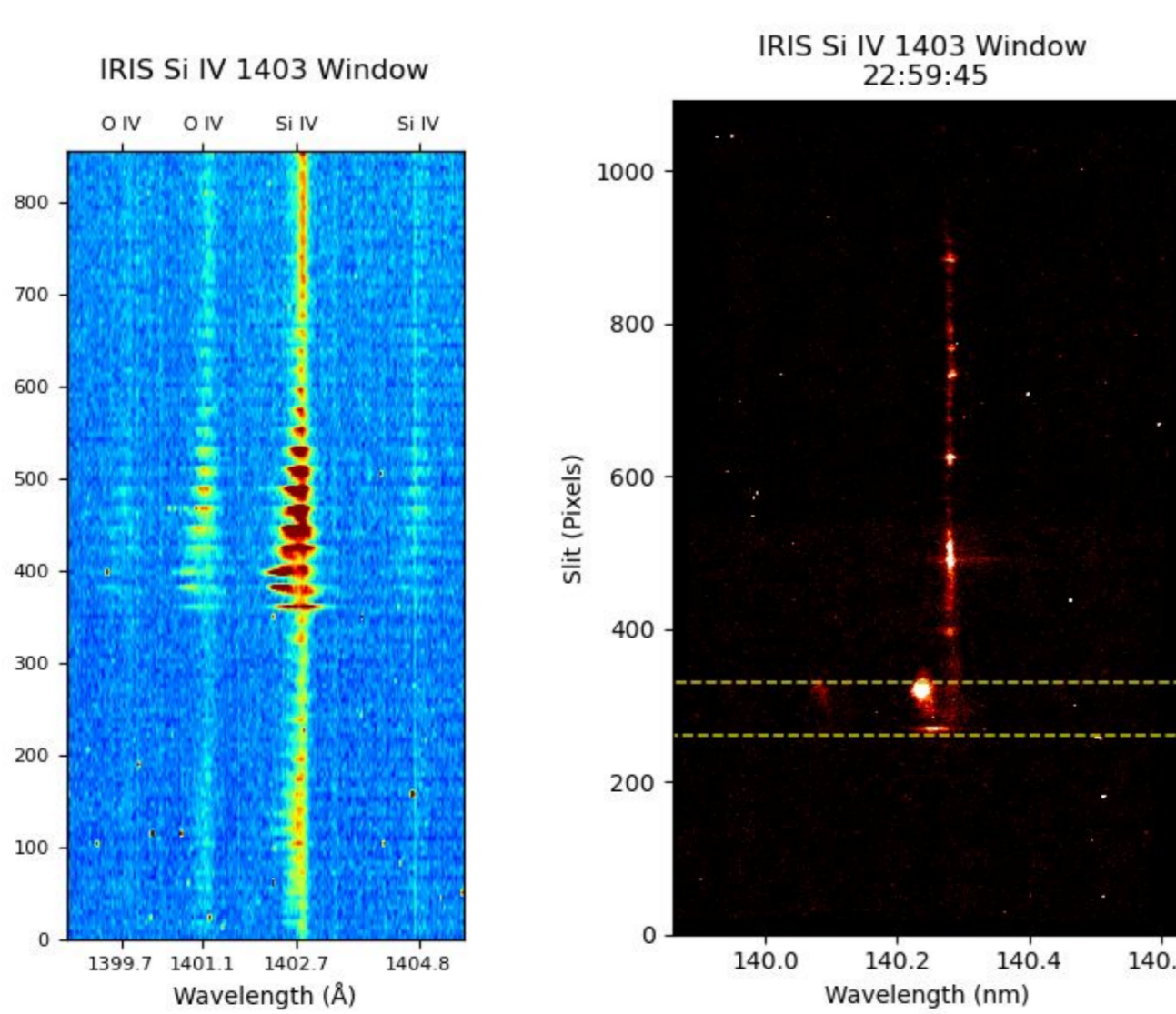


Figure 4: (a) O IV (1401.16 Å) and Si IV (1402.77 Å) line signatures during jet J2b, (b) Region taken for jet J2b for analysis of IRIS Si IV 1403 channel.

We applied single Gaussian fitting to the spectral lines and used the calculated intensity ratio to compare with the theoretical ratio-density curve, determining the electron density. (refer Fig 5 (a-d))

Results

Table 1: Different parameters derived for jets from IRIS and AIA data on 6 March 2022

| Jet | Velocity (v_{proj}) (km s ⁻¹) | | | Length (L) (Mm) | | | Width (w) (Mm) | | | Duration (t) (seconds) | | |
|-----|---|--------------|--------------|-----------------|------------|------------|----------------|-----------|-----------|------------------------|--------------|--------------|
| | 1400Å | 2796Å | 171Å | 1400Å | 2796Å | 171Å | 1400Å | 2796Å | 171Å | 1400Å | 2796Å | 171Å |
| J1 | 51.8 ± 7.5 | 54.0 ± 9.1 | 158.6 ± 33.0 | 4.6 ± 0.1 | 4.1 ± 0.1 | 15.3 ± 0.4 | 0.9 ± 0.1 | 0.9 ± 0.1 | 2.6 ± 0.4 | 88.7 ± 12.6 | 76.0 ± 12.6 | 96.0 ± 12.0 |
| J2a | 120.0 ± 9.8 | 51.1 ± 7.5 | 163.5 ± 10.4 | 12.7 ± 0.1 | 3.9 ± 0.1 | 31.8 ± 0.4 | 0.8 ± 0.1 | 0.7 ± 0.1 | 3.5 ± 0.4 | 118.6 ± 10.8 | 75.6 ± 10.8 | 194.2 ± 12.0 |
| J2b | 534.6 ± 33.1 | 248.7 ± 66.2 | 306.0 ± 23.4 | 35.7 ± 0.1 | 10.8 ± 0.1 | 48.3 ± 0.4 | 2.2 ± 0.1 | 1.6 ± 0.1 | 4.8 ± 0.4 | 108.0 ± 10.8 | 43.2 ± 10.8 | 157.8 ± 12.0 |
| J3 | 39.7 ± 3.4 | 38.2 ± 4.9 | 188.1 ± 26.9 | 6.0 ± 0.1 | 3.9 ± 0.1 | 16.1 ± 0.4 | 1.9 ± 0.1 | 1.2 ± 0.1 | 2.6 ± 0.4 | 152.0 ± 12.6 | 101.3 ± 12.6 | 85.6 ± 12.0 |

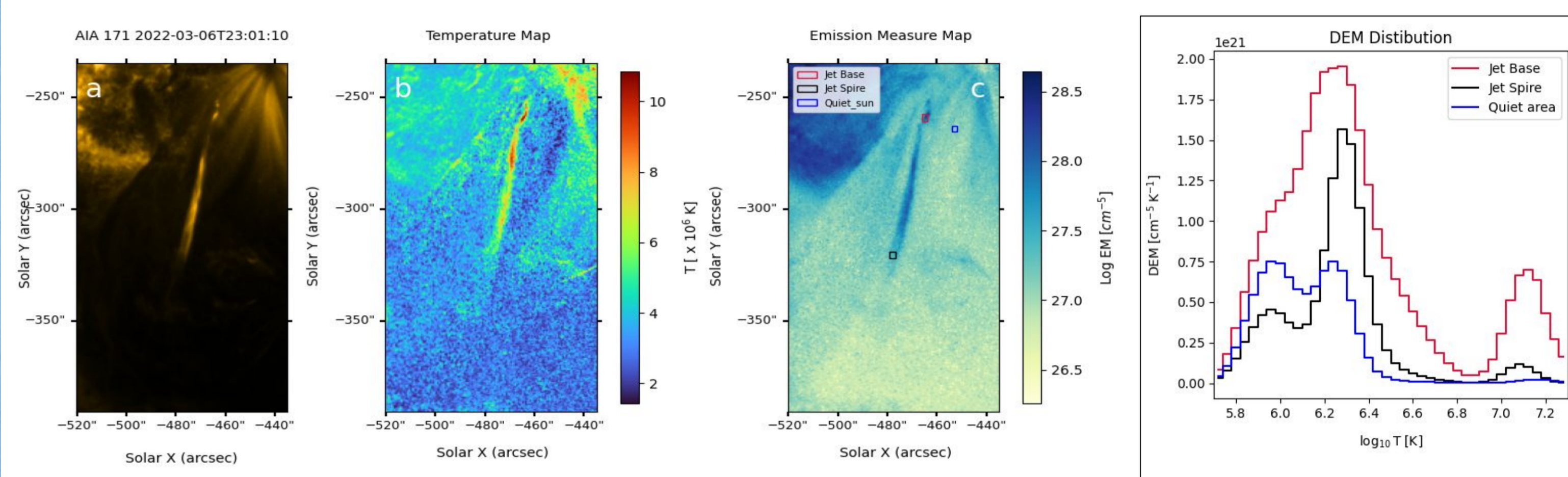


Table 2: Emission measure(EM), electron density(n_e) and energetic flux components for 4 jets

| Jet | EM (10 ²⁸ cm ⁻⁵) | | log(n_e) (cm ⁻³) | F_{kin} (10 ⁶ erg cm ⁻² sec ⁻¹) | F_{pot} (10 ⁶ erg cm ⁻² sec ⁻¹) | F_{enth} (10 ⁶ erg cm ⁻² sec ⁻¹) | F_{rad} (10 ⁶ erg cm ⁻² sec ⁻¹) |
|-----|---|-------|----------------------------------|---|---|--|---|
| | Base | Spire | Spire | | | | |
| J1 | 5.63 | 0.21 | 9.46 | 9.53 | 3.14 | 84.4 | 1.44 |
| J2a | 5.09 | 0.15 | 9.35 | 8.24 | 5.27 | 34.6 | 1.85 |
| J2b | 1.54 | 0.16 | 9.28 | 46.3 | 13.1 | 82.8 | 2.06 |
| J3 | 2.45 | 0.27 | 9.50 | 17.8 | 4.42 | 63.3 | 1.89 |

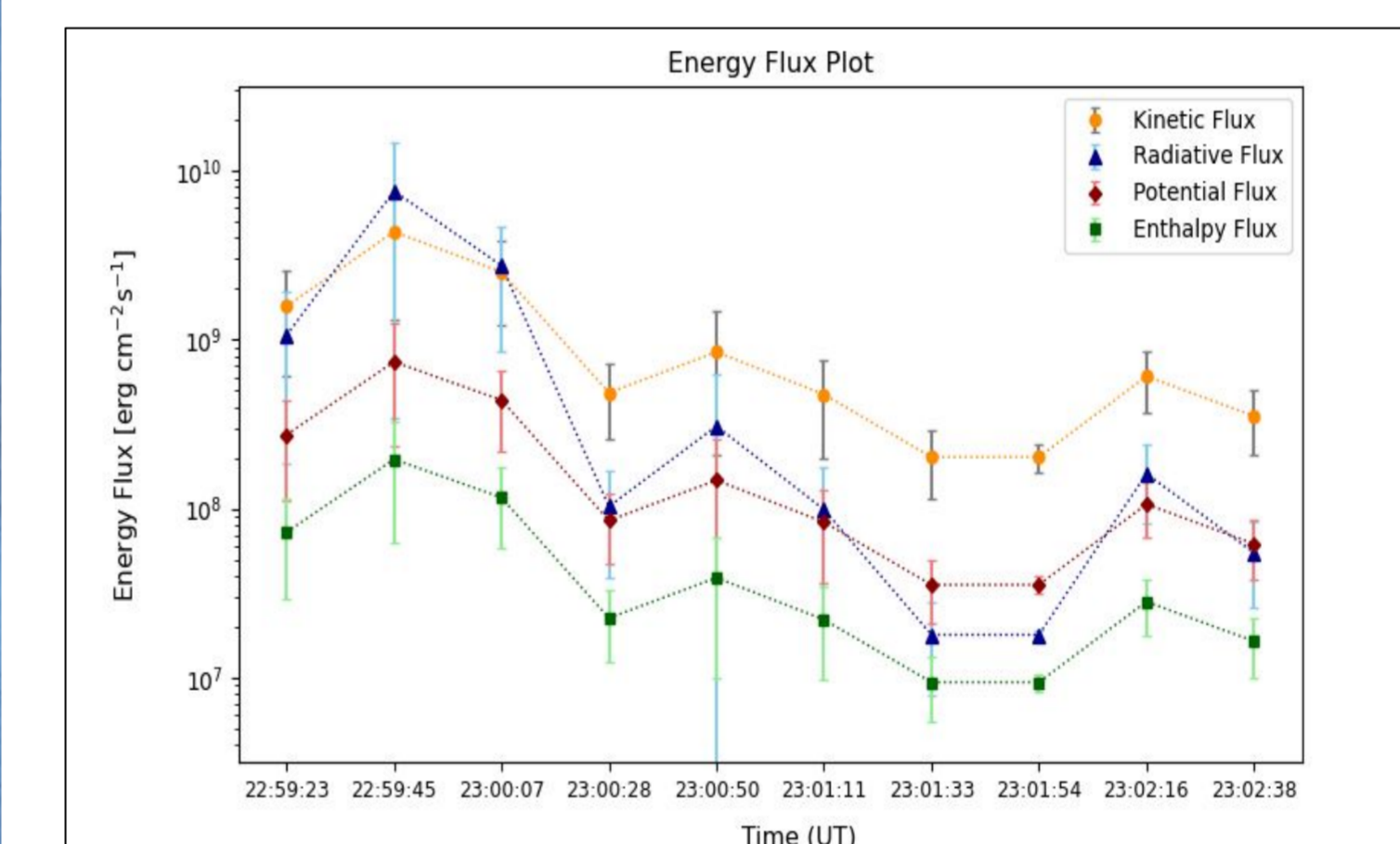


Figure 6: Variation of different energy fluxes for jet J2b

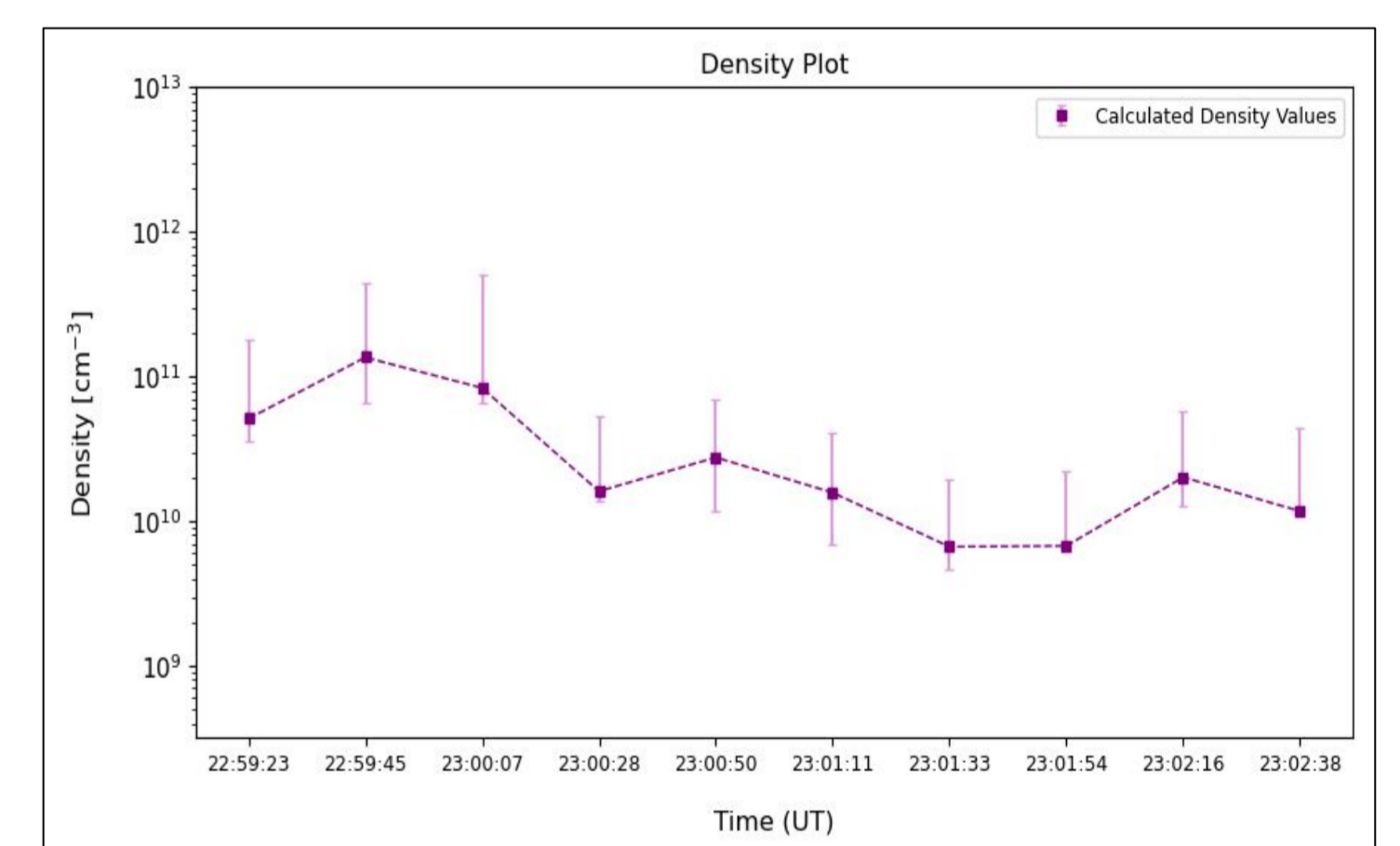


Figure 7: Variation of density for jet J2b spire

Conclusion & Key Takeaways

- ☐ From the DEM distribution, we identified a secondary peak for the base region at logT = 7.1, indicating the presence of very high temperatures. Such elevated temperatures at the base are likely a consequence of magnetic reconnection.
- ☐ The observed jets are multi-thermal, with temperatures of 6–9 MK at the base and 3–4 MK at the spire, as deduced from the DEM method.
- ☐ Total flux values ($\sim 10^8$ erg cm⁻² s⁻¹) are more than the coronal energy losses, indicating that the energy fluxes are sufficient enough to heat the corona locally.
- ☐ Largest contribution is by enthalpy flux followed by kinetic flux, where F_{enth} term appears to be 2-5 times more than the F_{kin} .

Future Plan

- ☐ We aim to analyze magnetic field dynamics near NOAA 12960, focusing on flux emergence, cancellation events, and the evolution of topology to identify key reconnection sites.
- ☐ Quantify the magnetic energy budget associated with jet formation.
- ☐ Study the multi-thermal plasma structure near jet J2b to identify eruption triggers.
- ☐ Examine the presence of pre-reconnection heating signatures and their relationship to the eruption dynamics.
- ☐ Analyze thermal and non-thermal emission signatures using *Solar Orbiter* and IRIS spectroscopic data.

Reference

- Hannah, I. G. and E. P. Kontar (Mar. 2012).
- Moore, Ronald L. et al. (Sept. 2010). "Dichotomy of Solar Coronal Jets: Standard Jets and Blowout Jets".
- Mulay, Sargam M. et al. (May 2016). "Multiwavelength study of 20 jets that emanate from the periphery of active regions"
- Paraschiv, A. R., A. Bemporad, and A. C. Sterling (July 2015). "Physical properties of solar polar jets. A statistical study with Hinode XRT data".
- Pucci, Stefano et al. (Oct. 2013). "Physical Parameters of Standard and Blowout Jets".
- Withbroe, G. L. and R. W. Noyes (Jan. 1977). "Mass and energy flow in the solar chromosphere and corona."

Digital Copy



Contact : prakhar@aries.res.in